Finite-Fixed Switching Predictive Control Technique for a 7-Level Cascaded H-Bridge Multilevel Active Power Filter. A Comparative Study

Raúl GREGOR, Jorge RODAS
Laboratory of Power and Control Systems
Facultad de Ingeniería, Universidad Nacional de Asunción
Luque, CP 2060, Paraguay
E-mail: rgregor@ing.una.py, jrodas@ing.una.py

ABSTRACT

This paper presents a finite-fixed predictive control technique applied to the three-wire cascade H-bridge multilevel converters for active power filter applications. The focus of this paper is to examine the impacts of the use of optimum modulation techniques combined with predictive current control in order to increase the control performance in terms of reactive power compensation and total harmonic distortion. The proposed approach predicts the future behavior of the control actions considering all possible switching states considering an increased prediction horizon in order to select the optimal switching vector by using an optimization process considering a defined cost function. Finally, the proposed control technique applies an optimum modulation technique. The effectiveness of the proposed control approach will be evaluated through simulations.

Keywords: Predictive control, cascade H-bridge converter, reactive power compensation, finite-fixed swiching.

1. INTRODUCCION

Recently, power quality has been consolidated as a scientific topic in the field of electrical engineering. Power quality is often defined as the electrical network's (or the grid's) ability to supply a clean and stable power. Actually, power factor (PF), voltage collapse, unbalance, excessive harmonics, transients and oscillations, have been a major concern in power transmission and distribution systems. Non-linear loads normally produce disturbances in power transmission and distribution systems, causing a high-level harmonic distortion in the phase currents and voltages. Moreover, reactive loads produce a low PF, causing an excessive reactive power (VAR) restricting the maximum active power transfer, adding losses to the power transmission and distribution systems affecting its stability and reliability [1]-[3]. Nowadays, several developments of flexible AC transmission system controllers, such as VAR compensators, have been successfully implemented to overcome the aforementioned drawbacks. In recent years, multilevel converters have become a popular alternative to overcome the technological restrictions of the actual semiconductors devices that have limited power ratings [4]. Among all multilevel topologies, the cascaded H-bridge (CHB) multilevel converter is often considered as one of the most suitable configuration for active power filter (APF), especially useful for reactive power compensation [5]. CHB converter-based APFs have been widely used in high-power applications due to its inherent advantages, such as reduced switching losses, higher conversion efficiency, modular structure, scalability to extended to more levels and higher number of redundant switching states [6]-[8]. Furthermore, in terms of control strategies, the CHB converter topology increases the degrees of freedom due to its modular feature which allows it to impose an asymmetric control approach. In the mentioned control method certain cells could compensate the PF associated with the fundamental frequency and other could control the current harmonic distortion [9], [10]. In this context, the main contribution of this paper compared to previous works will focus on providing a background material about the finite-fixed switching predictive control technique for a 7-level CHB multilevel APF.

The rest of this paper is organized as follows. Section 2 presents the mathematical model of the system. A detailed description of the proposed fixed switching predictive control strategy based on the model is given in Section 3. Simulation results are compared with the conventional predictive control strategy in Section 4. Concluding remarks are discussed and highlighted in the conclusion section.

2. CHB converter-based STATCOM model

The system under study is a three-phase 7-level CHB power converter depicted in Fig. 1. This system is used as STATCOM

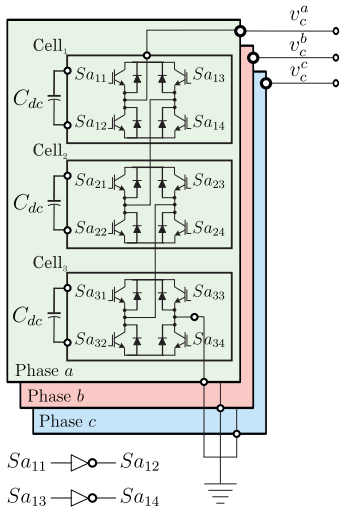

Fig. 1. Three-phase 7-level CHB converter.

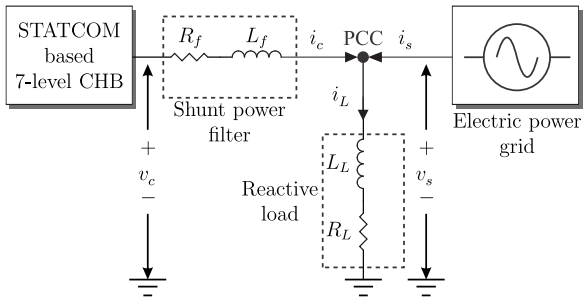

Fig. 2. STATCOM, load and electric grid connected through the PCC.

and it is coupled to reactive loads (Z_L) as well as to the power grid through a shunt power filter (L_f-R_f), connected at the PCC as shown in Fig. 2. The STATCOM is built by using three cells H-bridge per phase with an independent DC-link for each cell. Note that all DC-link buses have equals capacitances (C_{dc}) and the voltages (v_{dc}) values. Four power switching devices, typically IGBTs or SiC-MOSFETs [11]-[13], are used for each cells, where they are activated with firing signal $s\phi_{ij}$, being ϕ the corresponding phase (a, b or c), i the cell number (1, 2 or 3) and j the switching device (1, 2, 3 or 4). In order to avoid short-circuit in the DC-link the signals $s\phi_{i1}$ and $s\phi_{i4}$ are complementary to $s\phi_{i2}$ and $s\phi_{i4}$, respectively. Consequently, just $2n_c = 6$ signals are needed to control output voltages (v_c^ϕ). Each phase has $n_c = 3$ number of cells and $\varepsilon = 2^{2n_c} = 64$ possible switching states. Next, each switching state corresponds to the following switching function:

$$F_s^\phi = \sum_{i=1}^{n_c} F_i^\phi \tag{1}$$

being F_i^ϕ the switching function for the cell i. The output voltage can be synthesized as a function of the DC-link voltage v_{dc} and the switching function F_s^ϕ as:

$$v_c^\phi = F_s^\phi v_{dc}. \tag{2}$$

Using Kirchhoff's circuit laws, the continuous time-domain model of the CHB converter-based STATCOM is:

$$\frac{\mathrm{d}i_c^\phi}{\mathrm{d}t} = \frac{v_s^\phi}{L_f} - \frac{R_f}{L_f} i_c^\phi - \frac{v_c^\phi}{L_f} \tag{3}$$

where i_c^ϕ is the current injected by the CHB converter-based STATCOM and v_s^ϕ the grid voltage. The discrete time-domain model is obtained by using the forward-Euler discretization method:

$$i_c^\phi(k+1) = \left(1 - \frac{R_f T_s}{L_f}\right) i_c^\phi(k) + \frac{T_s}{L_f}\left\{v_s^\phi(k) - v_c^\phi(k)\right\} \tag{4}$$

being T_s the sampling time, k identifies the actual discrete-time sample and $i_c^\phi(k+1)$ are the predictions of the STATCOM phase currents made at sample k.

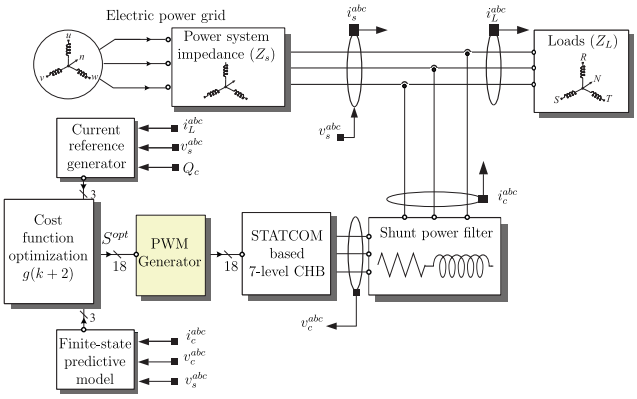

Fig. 3. Proposed finite-fixed switching predictive current controller technique for a 7-level CHB APF.

3. Proposed controller

First, the controller uses the discrete-time model of the system represented by (4) in order to evaluate its future behavior for each possible switching states. Then, by using an user-defined cost function, the optimal switching state (the one that minimizes the cost function) is applied during the next sampling time. This procedure is known as model-based predictive control and has been applied with success in power converters such as conventional 2-level voltage source inverter [14], matrix converters [15]-[17], multiphase machines [18]-[21], multiphase generators [22]-[24], among others. As this procedure takes time comparable with the sampling time, a second-ahead prediction is needed. In this work, a quadratic measure of the predicted error (J) is evaluated a cost function typically defined as:

$$J = J(k+2) = \| \Delta i_c(k+2) \|^2 \tag{5}$$

where the predicted current error is:

$$\Delta i_c(k+1) = i_c^*(k+2) - i_c(k+2) \tag{6}$$

and the subscript (*) denotes the reference variables. As can be seen in (6), the proposed algorithm needs to be calculating the STATCOM instantaneous current reference.

A. Current reference generator

To allow an unitary power factor at the grid side, the instantaneous active (P_c^*) and reactive (Q_c^*) power references are defined as follows:

$$P_c^* = 0 \tag{7}$$

$$Q_c^* = -Q_L \tag{8}$$

The reactive power at the load side can be written as:

$$Q_L = v_{s\beta} i_{L\alpha} - v_{s\alpha} i_{L\beta} \tag{9}$$

where $v_{s\alpha}$ and $v_{s\beta}$ denote the voltage signals from the grid side and $i_{L\alpha}$ and $I_{L\beta}$ are the currents in the load side in the stationary reference frame (α - β). Equations (7) and (8) highlight the main

goal of the STATCOM, which is to achieve zero consumption of reactive power from the grid side. Current references are calculated from the following equations:

$$i^*_{c\alpha} = \frac{2}{3}\,\frac{v_{s\alpha}}{v^2_{s\alpha}+v^2_{s\beta}}\,P^*_c + \frac{2}{3}\,\frac{v_{s\beta}}{v^2_{s\alpha}+v^2_{s\beta}}\,Q^*_c \tag{10}$$

and

$$i^*_{c\beta} = \frac{2}{3}\,\frac{v_{s\beta}}{v^2_{s\alpha}+v^2_{s\beta}}\,P^*_c - \frac{2}{3}\,\frac{v_{s\alpha}}{v^2_{s\alpha}+v^2_{s\beta}}\,Q^*_c \tag{11}$$

STATCOM phase currents references used in the optimization process are:

$$i^{abc^*}_c = \mathbf{T}^{-1}[i^*_{c\alpha} \;\; i^*_{c\beta} \;\; 0]^{'} \tag{12}$$

where the superscript ($^{'}$) indicates the transposed matrix and $\mathbf{T}$ is the Clarke transformation matrix:

$$\mathbf{T} = \sqrt{\frac{2}{3}}\begin{bmatrix} 1 & -\frac{1}{2} & -\frac{1}{2} \\ 0 & \frac{\sqrt{3}}{2} & -\frac{\sqrt{3}}{2} \\ \frac{1}{\sqrt{2}} & \frac{1}{\sqrt{2}} & \frac{1}{\sqrt{2}} \end{bmatrix} \tag{13}$$

B. Cost function optimization

The cost function optimization is performed by exhaustive search over all possible switching vectors of the control action. During the optimization process, both, the cost function (5) and the predictive model must be computed 64 times at each sampling period to guarantee optimality, since there are 64 possible switching vectors for this case of study. These switching vectors represent all possible output voltages of the STATCOM, v^a_c, v^b_c and v^c_c, connected at the PCC. The output voltages can be represented by:

$$\begin{bmatrix} v^a_c \\ v^b_c \\ v^c_c \end{bmatrix} = \begin{bmatrix} v_{c1} \\ v_{c2} \\ v_{c3} \end{bmatrix} v_{dc} \tag{14}$$

where v_{c1}, v_{c2} and v_{c3} are the optimal levels of the three-phase 7-level CHB converter-based STATCOM system $(-3,-2,-1,0,1,2,3)$. The first 10 switching vectors for one phase (a) are shown in Table I.

TABLE I
FIRST 10 SWITCHING VECTORS FOR A THREE-PHASE 7-LEVEL CHB CONVERTER-BASED STATCOM SYSTEM

$S_{a_{ij}}$						η	v^a_c value
Sa_{11}	Sa_{13}	Sa_{21}	Sa_{23}	Sa_{31}	Sa_{33}		
0	0	0	0	0	0	1	0
0	0	0	0	0	1	2	-1
0	0	0	0	1	0	3	1
0	0	0	0	1	1	4	0
0	0	0	1	0	0	5	-1
0	0	0	1	0	1	6	-2
0	0	0	1	1	0	7	0
0	0	0	1	1	1	8	-1
0	0	1	0	0	0	9	1
0	0	1	0	0	1	10	0
.	.	.	.	.	.	.	.
.	.	.	.	.	.	.	.
.	.	.	.	.	.	.	.

Algorithm 1 Optimization algorithm

1. Initialize $J^a_o := \infty, J^b_o := \infty, J^c_o := \infty, \eta := 0$
2. Compute the STATCOM reference currents. Eqn. (12).
3. **while** $\eta \leq \varepsilon$ **do**
4. $\quad S_{f_{ij}} \leftarrow S^{\eta}_{f_{ij}} \;\; \forall\; i \;\&\; j = 1,\; 2,\; 3$
5. $\quad$ Compute the STATCOM prediction currents.
6. $\quad$ Compute the dynamics of the DC side. Eqn. (14).
7. $\quad$ Compute the predicted current error. Eqn. (6).
8. $\quad$ Compute the cost function. Eqn. (5).
9. $\quad$ **if** $J^a < J^a_o$ **then**
10. $\quad\quad J^a_o \leftarrow J^a, \;\; S^{opt}_a \leftarrow S_{a_{ij}}$
11. $\quad$ **end if**
12. $\quad$ **if** $J^b < J^b_o$ **then**
13. $\quad\quad J^b_o \leftarrow J^b, \;\; S^{opt}_b \leftarrow S_{b_{ij}}$
14. $\quad$ **end if**
15. $\quad$ **if** $J^c < J^c_o$ **then**
16. $\quad\quad J^c_o \leftarrow J^c, \;\; S^{opt}_c \leftarrow S_{c_{ij}}$
17. $\quad$ **end if**
18. $\quad \eta := \eta + 1$
19. **end while**
20. Compute the PWM duty cycles. Eqn. (15).

Finally, the optimization algorithm selects the optimum vector S^{opt} that minimizes the defined cost function represented by (5). Algorithm 1 summarizes the optimization process.

C. PWM duty cycles calculation

The CHB STATCOM duty cycles calculation of the proposed algorithm proceeds as follows. For a desired instantaneous active and reactive power references, the control algorithm determines the optimal vector (S^{opt}_f) that minimizes (5). The optimal vector provides the optimum voltages ($v^{a,opt}_c$, $v^{b,opt}_c$, $v^{c,opt}_c$) in terms of the CHB STATCOM current and voltage errors, respectively. Instead of applying the selected voltage vector to the CHB STATCOM during the whole switching period, which is the standard procedure in conventional predictive control schemes, the proposed algorithm uses S^{opt}_f to calculate the duty cycles by using the following equation:

$$\begin{bmatrix} \tau_a \\ \tau_b \\ \tau_c \end{bmatrix} = \frac{1}{3}(v^{-1}_{dc})[v^{a,opt}_c \;\; v^{b,opt}_c \;\; v^{c,opt}_c]^{'} \tag{15}$$

where τ_f is the duty cycles vector and the subscript $f = a, b, c$ are associated with the CHB STATCOM phase voltages and are normalized between -1 and 1. The calculation of the duty cycles is proposed as an optimization problem aimed to minimize the prediction error. This procedure can be considered as a systematic application in one sampling period of the optimal combination of more than one vector to minimize the CHB STATCOM current errors in the AC side and the capacitor voltage errors in the DC side, respectively.

4. Simulation results

A MatLab/Simulink simulation environment has been developed to analyze the performance of the proposed finite-fixed predictive controller applied to the three-phase 7-level CHB converter-based APF, considering the electrical parameters shown in

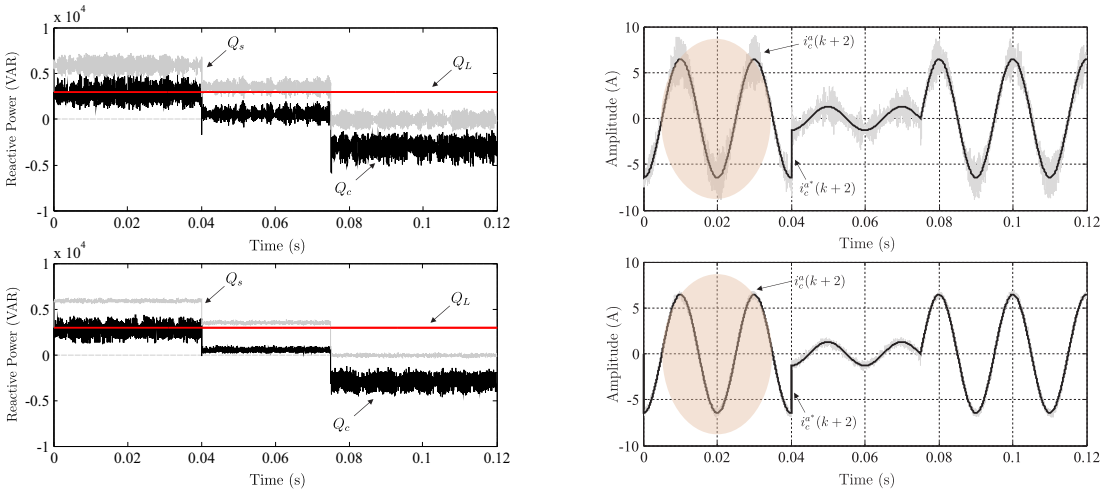

(a) Reactive power reference and compensation.

(b) Current Tracking.

Fig. 4. CHB APF comparison performance.

Table II. Numerical integration using Runge-Kutta method has been applied to compute the evolution of the variables step by step in the time domain. The performance of the proposed predictive control method has been analyzed in terms of reactive power compensation as well as total harmonic distortion (THD) of the grid side currents, Eqn. (16) and mean squared error (MSE), Eqn. (17), considering a 40 kHz of the sampling frequency and setting 114 V in the DC side.

$$\text{THD} = \sqrt{\frac{1}{i_1^2}\sum_{i=2}^{N} i_i^2} \tag{16}$$

$$\text{MSE}(\Psi) = \sqrt{\frac{1}{N}\sum_{j=1}^{N} \Psi_j^2} \tag{17}$$

where N is the number of vector elements, i_1 is the amplitude of the fundamental frequency of the analyzed current, and i_i are the current harmonics.

TABLE II
PARAMETERS DESCRIPTION

	7-Level CHB APF		
PARAMETER	SYMBOL	VALUE	UNIT
Electric frequency of the grid	f_e	50	Hz
Voltage of the electric grid	v_s	310.2	V
Filter resistance	R_f	0.09	Ω
Filter inductance	L_f	3	mH
DC-link voltage	v_{dc}	114	V
	Load parameters		
Load resistance	R_L	23.2	Ω
Load inductance	L_L	55	mH
	Predictive control parameters		
Sampling time	T_s	66	μs
Active power reference	P_c^*	0	W
Ideal Reactive power reference	Q_c^*	$-Q_L$	VAR

Fig. 4 shows simulation results performed in order to analyze the feasibility of the proposed control technique under steady-state and transient conditions. For comparison purposes in the upper figures are shown the results obtained by the classical predictive control method without modulation, and in the bottom figures are shown the results obtained by the proposed finite-fixed predictive control method. Fig. 4 (a) shows a multi-step in the instantaneous reactive power reference where is possible to notice the effect of reactive power compensation. Moreover, Fig. 4 (b), shows the tracking current dynamic performance for a step change of the reactive power reference considering both control methods. From these figures can be quantified an improvement in terms of the MSE about 73 % (a reduction from 0.98 to 0.27) if is considered the proposed method.

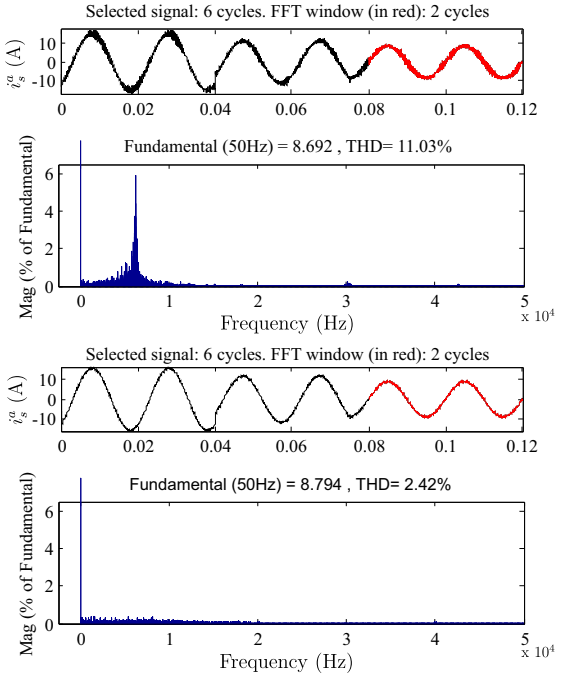

Fig. 5. THD of the grid current.

Finally, Fig. 5 shows the total harmonic distortion (THD) behavior of the grid current (i_s^a). It can be observed from the simulation results that the THD is reduced from 11 % to 2.42 % if is considered the proposed finite-fixed predictive control technique.

5. Conclusion

In this paper, a predictive current control technique combined with a modulation stage in order to avoid the variable switching frequency inherent in conventional predictive controllers is applied to a CHB multilevel STATCOM converter. Simulation results show that it is possible to combine the use of predictive control with modulation techniques to obtain better performance than the classic predictive control approach and confirm the capability of the proposed finite-fixed predictive control technique to compensate the instantaneous reactive power. Simulation results also verify that the proposed control technique can be viable especially in terms of lower THD and MSE of the grid currents side. Obtained results confirm that maintaining the modulation technique easing the switch selection and providing a more adequate harmonic profile.

Acknowledgments

The authors would like to thank the Paraguayan Government for their encouragement and kind financial support provided through the CONACYT grant project (14-INV-097).

6. REFERENCES

[1] S. H. Jo, S. Son and J. W. Park, "On Improving Distortion Power Quality Index in Distributed Power Grids," **IEEE Transactions on Smart Grid**, vol. 4, no. 1, pp. 586–595, Mar. 2013.

[2] L. K. Haw, M. S. A. Dahidah and H. A. F. Almurib, "A New Reactive Current Reference Algorithm for the STATCOM System Based on Cascaded Multilevel Inverters," **IEEE Transactions on Power Electronics**, vol. 30, no. 7, pp. 3577–3588, Jul. 2015.

[3] Y. Neyshabouri, H. Iman-Eini and M. Miranbeigi, "State feedback control strategy and voltage balancing scheme for a transformerless STATic synchronous COMpensator based on cascaded H-bridge converter," **IET Power Electronics**, vol. 8, no. 6, pp. 906–917, Jun. 2015.

[4] J. Muñoz, et al, "Static Compensators (STATCOMs) in Power Systems," **Control of Multilevel STATCOMs**, ISBN:978-981-287-281-4, pp. 265–311, 2015.

[5] A. Marzoughi, Y. Neyshabouri and H. Imaneini, "Control scheme for cascaded H-bridge converter-based distribution network static compensator," **IET Power Electronics**, vol. 7, no. 11, pp. 2837–2845, Nov. 2014.

[6] C. D. Townsend, T. J. Summers and R. E. Betz, "Phase-Shifted Carrier Modulation Techniques for Cascaded H-Bridge Multilevel Converters," **IEEE Transactions on Industrial Electronics**, vol. 62, no. 11, pp. 6684–6696, Nov. 2015.

[7] Y. Yu, G. Konstantinou, B. Hredzak and V. G. Agelidis, "Operation of Cascaded H-Bridge Multilevel Converters for Large-Scale Photovoltaic Power Plants Under Bridge Failures," **IEEE Transactions on Industrial Electronics**, vol. 62, no. 11, pp. 7228–7236, Nov. 2015.

[8] G. Farivar, B. Hredzak and V. G. Agelidis, "Decoupled Control System for Cascaded H-Bridge Multilevel Converter Based STATCOM," **IEEE Transactions on Industrial Electronics**, vol. 63, no. 1, pp. 322–331, Jan. 2016.

[9] X. Li, M. Su, Y. Sun, H. Dan and W. Xiong, "Modulation Strategy Based on Mathematical Construction for Matrix Converter Extending the Input Reactive Power Range," **IEEE Transactions on Power Electronics**, vol. 29, no. 2, pp. 654–664, Feb. 2014.

[10] L. Sun, Z. Wu, F. Xiao, X. Cai and S. Wang, "Suppression of Real Power Back Flow of Nonregenerative Cascaded H-Bridge Inverters Operating Under Faulty Conditions," **IEEE Transactions on Power Electronics**, vol. 31, no. 7, pp. 5161–5175, Jul. 2014.

[11] J. Pacher, J. Rodas, R. Gregor, M. Rivera, A. Renault, L. Comparatore, "Efficiency Analysis of a Modular H-Bridge based on SiC MOSFET," **International Journal of Electronics Letters**, Early access, pp. 1–9, 2018.

[12] E. Maqueda, S. Toledo, R. Gregor, D. Caballero, F. Gavilan, J. Rodas, M. Rivera, P. Wheeler, "An Experimental Implementation of Predictive Control in Direct Matrix Converter based on SiC MOSFET Bidirectional Switches," in **Proc. IEEE Southern Power Electronics Conference: SPEC 2017**, Puerto Varas, Chile, 2017.

[13] S. Toledo, E. Maqueda, M. Rivera, R. Gregor, D. Caballero, F. Gavilan, J. Rodas, "Experimental Assessment of IGBT and SiC-MOSFET based Technologies for Matrix Converter using Predictive Current Control," in **Proc. IEEE CHILECON**, Pucon, Chile, 2017.

[14] D. Caballero, F. Gavilan, R. Gregor, J. Rodas, S. Toledo, J. Rodriguez-Pineiro, "MBPC Power Control in Three-Phase Inverters for Grid-Connected Applications," in **Proc. IEEE Conference on Innovative Smart Grid Technologies - Latin America: ISGT-LA**, Montevideo, Uruguay, pp. 817–821, 2015.

[15] D. Caballero, F. Gavilan, E. Maqueda, R. Gregor, J. Rodas, D. Gregor, S. Toledo, M. Rivera, "Active and Reactive Power Control Strategy for Grid-Connected Six-Phase Generator by Using Multi-Modular Matrix Converters," **Journal on Systemics, Cybernetics and Informatics**, vol. 14, no. 6, pp. 57–61, 2016.

[16] S. Toledo, M. Rivera, R. Gregor, J. Rodas, L. Comparatore, "Predictive Current Control with Reactive Power Minimization in Six-Phase Wind Energy Generator using Multi-Modular Direct Matrix Converter," in **Proc. IEEE Andean Council International Conference: ANDESCON**, Arequipa, Peru, 2016.

[17] S. Toledo, R. Gregor, M. Rivera, J. Rodas, D. Gregor, D. Caballero, F. Gaviln, E. Maqueda, "Multi-Modular Matrix Converter Topology applied to Distributed Generation Systems," in **Proc. IET International Conference on Power Electronics, Machines and Drives: PEMD 2016**, Glasgow, Scotland, 2016.

[18] J. Rodas, R. Gregor, M. Rivera, Y. Takase, M. Arzamendia, "Efficiency Analysis of Reduced-Order Observers applied to the Predictive Current Control of Asymmetrical Dual Three-Phase Induction Machines," in **Proc. Symposium on Predictive Control of Electrical Drives and Power Electronics: PRECEDE**, Munich, Germany, pp. 1–7, 2013.

[19] R. Gregor, J. Rodas, "Speed Sensorless Control of Dual Three-Phase Induction Machine based on a Luenberger Observer for Rotor Current Estimation," in **Proc. Annual Conference of the IEEE Industrial Electronics Society: IECON**, Montreal, Qc, Canada, pp. 3653–3658, 2012.

[20] J. Rodas, F. Barrero, M.R. Arahal, C. Martn, R. Gregor, "On-Line Estimation of Rotor Variables in Predictive Current Controllers: a Case Study using Five-Phase Induction Machines," **IEEE Transactions on Industrial Electronics**, vol. 63, no. 9, pp. 5348–5356, Sep. 2016.

[21] J. Rodas, C. Martin, M.R. Arahal, F. Barrero, R. Gregor, "Influence of Covariance-Based ALS Methods in the Performance of Predictive Controllers with Rotor Current Estimation," **IEEE Transactions on Industrial Electronics**, vol. 64, no. 4, pp. 2602–2607, Apr. 2017.

[22] J. Rodas, H. Guzman, R. Gregor, F. Barrero, "Model Predictive Current Controller using Kalman Filter for Fault-Tolerant Five-Phase Wind Energy Conversion Systems," in **Proc. IEEE International Symposium on Power Electronics for Distributed Generation Systems: PEDG**, Vancouver, BC, Canada, 2016.

[23] J. Rodas, R. Gregor, Y. Takase, D. Gregor, D. Franco, "Multi-Modular Matrix Converter Topology applied to the Six-Phase Wind Energy Generator," in **Proc. International Universities Power Engineering Conference: UPEC 2015**, Stoke-on-Trent, England, pp. 1–6, 2015.

[24] J. Rodas, R. Gregor, Y. Takase, H. Moreira, M. Rivera, "A Comparative Study of Reduced Order Estimators applied to the Speed Control of Six-Phase Generator for a WT Applications," in **Proc. Annual Conference of the IEEE Industrial Electronics Society: IECON**, Vienna, Austria, pp. 5124–5129, 2013.